Available online at www.sciencedirect.com
SCIENCE DIRECT
Biochemical and Biophysical Research Communications 345 (2006) 430–437
BBRC
www.elsevier.com/locate/ybbrc

3D modeling of the activated states of constitutively active mutants of rhodopsin ☆

Gregory V. Nikiforovich *, Garland R. Marshall

Department of Biochemistry and Molecular Biophysics, Washington University School of Medicine, St. Louis, MO 63110, USA

Received 27 March 2006
Available online 25 April 2006

Abstract

The activated (R*) states in constitutively active mutants (CAMs) of G-protein-coupled receptors (GPCRs) are presumably characterized by lower energies than the resting (R) states. If specific configurations of TM helices differing by rotations along the long transmembrane axes possess energies lower than that in the R state for pronounced CAMs, but not for non-CAMs, these particular configurations of TM helices are candidate 3D models for the R* state. The hypothesis was studied in the case of rhodopsin, the only GPCR for which experimentally determined 3D models of the R and R* states are currently available. Indeed, relative energies of the R* state were significantly lower than that of the R state for the rhodopsin mutants G90D/M257Y and E113Q/M257Y (strong CAMs), but not for G90D, E113Q, and M257Y (not CAMs). Next, the developed build-up procedure successfully identified few similar configurations of the TM helical bundle of G90D/M257Y and E113Q/M257Y as possible candidates for the 3D model of the R* state of rhodopsin, all of them being in good agreement with the model suggested by experiment. Since constitutively active mutants are known for many of GPCRs belonging to the large rhodopsin-like family, this approach provides a way for predicting possible 3D structures corresponding to the activated states of the TM regions of many GPCRs for which CAMs have been identified.

Keywords: G-protein-coupled receptor; Rhodopsin; Constitutively active mutants; Molecular modeling; Transmembrane region

G-protein-coupled receptors (GPCRs) comprise a vast protein family with more than 800 members [1,2] that are involved in a variety of physiological functions. They represent about 50% of the targets for drugs currently in use [3]. These receptors are integral membrane proteins, and include seven helical transmembrane (TM) stretches as well as non-TM parts, namely the N- and C-terminal fragments and the extra- and intracellular loops connecting the TM helices. GPCRs, in general, serve to transform an extracellular event, typically binding of a ligand (neurotransmitter, peptide hormone, etc.), to an intracellular signal, such as cyclic AMP, via heterotrimeric GTP-binding proteins.

During the process of transduction G-protein-coupled receptors undergo conformational transitions from their resting states (the R states) to the activated states (the R* states). It is reasonable to hypothesize that R and R* do not differ significantly in their relative energies. Indeed, transfer from R to R* is initiated by binding of a ligand that is normally of much smaller size than the GPCR; therefore, structural perturbations due to ligand binding cannot force a GPCR to adopt a conformation of significantly higher overall energy. This should be especially true for constitutively active mutants (CAMs) that display functional activity even in the absence of perturbations from the ligand (basal activity). In fact, many authors have adopted the view that conformational transfer from R to R* in CAMs is initiated by elimination of some constraints existing in R, thus releasing the R* state (see, e.g., [4]); it

☆ *Abbreviations:* GPCR, G-protein-coupled receptor; CAM, constitutively active mutant; TM, transmembrane helix; 3D, three-dimensional; PDB, Protein Data Bank.

* Corresponding author. Fax: +1 314 362 0234.
E-mail address: gregory@ccb.wustl.edu (G.V. Nikiforovich).

0006-291X/$ - see front matter © 2006 Elsevier Inc. All rights reserved.
doi:10.1016/j.bbrc.2006.04.058

implies that R* generally possesses a relative lower energy than that of R in the absence of internal stabilizing constraints.

Another reasonable assumption is that the 3D structures of the R* states for different CAMs of the same GPCR are similar to each other (see also discussion on advantages and disadvantages of employing CAMs as models for the R* states of GPCRs [4]). These 3D structures would presumably possess relative energy lower to that of the R state for each specific CAM, respectively. One possible approach, therefore, to elucidate tentative R* states is to determine all low-energy conformations for several pronounced CAMs of a given GPCR and compare them with each other. 3D structures that are geometrically similar and possess relative energies lower than those of the R states for all pronounced CAMs should be good candidates for the R* states.

This paper examines the above assumptions for the case of rhodopsin, the 348-residue seven-transmembrane α-helical photoreceptor of the visual system. Rhodopsin was chosen as an obvious test case, since experimental 3D models for both resting and activated states of a GPCR are available only for rhodopsin. The 3D structures of dark-adapted rhodopsin (the R state) have been determined by X-ray crystallography [5–9], and the structure of the transmembrane (TM) region of rhodopsin in the light-adopted state (the R* state) was deduced from data on site-directed spin labeling [10]. Recently, the structure of the MI state of rhodopsin, which is the transition state preceding the activated R* state (the MII state), was investigated by electron crystallography [11]. On the other hand, several CAMs of rhodopsin are well characterized in the literature [12–14].

Roughly, the TM helical bundle of rhodopsin in the R* state (the MII state) differs from that in the R state by rotation of the TM6 helix along the long transmembrane axis by ca. 120°; all other movements of TM helices upon rhodopsin activation suggested by the experimental data, such as movements of TM1, TM2, TM3, and TM7, are much smaller [10]. The largest GPCR family (family A, up to 700 members) displays distinct sequential homology to rhodopsin [1,2], and the X-ray structure of rhodopsin has been used as templates for building 3D structures of other rhodopsin-like GPCRs in their inactive states (see, e.g., a minireview [15]). There are also indications that the R* state involves similar types of rotations of TM6 not only in rhodopsin [16], but in β2-adrenoreceptor [17–19], parathyroid hormone receptor [20] or 5HT1 receptor [20,21] as well. The rotation of TM6 similar to that in rhodopsin was proposed as a "central dogma" of GPCR activation [22]. Other experimental data, however, were interpreted in favor of changes in mutual orientations of TM3 and TM7 (β2-adrenoreceptor [23], tachykinin NK-1 receptor [24], α(1β) adrenergic receptor [25], the complement factor 5a receptor [26], or TM2 and TM7 tachykinin NK-2 receptor [27]), or TM6 and TM7 (thyrotropin receptor [28]), or TM2 (angiotensin receptor type 1[29]); see also discussion on various models for R* [21]. A reasonable hypothesis, therefore, would be that, in the first rough assumption, conformational transitions from R to R* in GPCRs in general may be characterized by various rotations of TM helices along their long transmembrane axes.

To elucidate configurations of the TM bundle with energies lower than that for the rhodopsin-like R state that differ by rotations along their long axes, one needs to perform comprehensive sampling of the entire configurational space. GPCRs together with their environment (surrounding lipid and water molecules, ions, etc.) are, however, extremely large molecular systems. Thorough conformational sampling for such systems is clearly beyond the reach of currently available computational resources. For example, straightforward molecular dynamics (MD) simulations performed for rhodopsin starting from the R state covered a trajectory of only ca. 40 ns [30], whereas experiment estimates the time of transfer from R to R* (specifically, to the MII state) as milliseconds [31]. To overcome this fundamental obstacle, our study developed a build-up approach that allows prediction of 3D structures corresponding to configurations of the TM regions of GPCRs with energies lower than that of the rhodopsin-like R state by applying a simple and computationally inexpensive modeling procedure. The early version of this modeling approach has been used previously to study the R* state of rhodopsin [32].

Methods

Energy calculations. Generally, packing of TM helices of rhodopsin and its mutants into helical bundles was performed in the multidimensional space of parameters that included the "global" parameters (those related to movements of individual TM helices as rigid bodies, namely, their translations along the coordinate axes *X*, *Y*, *Z* and rotations around these axes Tx, Ty, and Tz) and the "local" parameters (internal dihedral rotational angles). The coordinate system for the global parameters was selected as follows: the long transmembrane axial *X* coordinate axis for each TM helix has been directed from the first to the last C^{α}-atom of the helix; the *Y* axis was perpendicular to *X* and went through C^{α}-atom of the "middle" residue of each helix; and the *Z* axis was built perpendicular to *X* and *Y* to maintain the right-handed coordinate system. For this purpose, boundaries of TM helices in Rh were defined as in the previous study [32], namely as follows: TM1, W35-M49-Q64 (the first, middle, and last residue, respectively); TM2, L72-F85-L99; TM3, T108-I123-V139; TM4, E150-W161-L172; TM5, N200-F212-Q225; TM6, A246-F261-T277; and TM7, I286-K296-Y306. The ECEPP/2 force field with rigid valence geometry [33,34] was used for all energy calculations; a distance cut-off of 8 Å was used for non-bonded interactions. Residues of Arg, Lys, Glu, and Asp were present as charged species with the standard ECEPP/2 value of macroscopic dielectric constant of 2.0. Since two sequential proline residues in TM5 (fragment 169–172, APPL) cannot be tolerated in a helix, P171 was replaced by alanine. The side chain of K296 was bonded to retinal through a Schiff base with its ε-amino group. The valence structure of 11-*cis* retinal was borrowed from the PDB entry 1F88; the partial charge of 0.640 was assigned to the nitrogen of the Schiff base. Explicit water and lipid molecules were omitted in the calculations.

First, each individual TM helix was subjected to energy minimization starting from the values of dihedral angles in the backbone corresponding to those in the PDB entry 1F88. All dihedral angles were allowed to rotate with the limitation $-20° \geqslant \phi, \psi \geqslant -100°$ that mimics, to some extent, limitations on intrahelical mobility of TM segments immobilized in the membrane, in accord with known X-ray data on TM helices [5,35,36]. For the same reason, the ω angles in the Pro residues were limited to the values $-150° \geqslant \omega \geqslant 150°$. Side-chain rotational angles were optimized before and after energy minimization by an algorithm developed earlier [37]. The dihedral angles of retinal and K296 were allowed to change during energy minimization, but they were not optimized prior to minimization (except the last C^5—C^6—C^7—C^8 angle in retinal). For mutant rhodopsin receptors, each TM helix containing a mutation was re-minimized individually.

After energy minimization for each individual helix, the seven TM helices were assembled in the bundle by assigning six "global" parameters to each helix as a rigid body, and energy calculations were performed for each starting configuration of the TM bundle (i.e., for each starting combination of the global parameters *X*, *Y*, *Z*, Tx, Ty, and Tz). Routinely, minimization of the energy of atom–atom interactions in the helical bundle was performed involving both global and local coordinates. The side-chain dihedral rotational angles were optimized before and after overall energy minimization. To decrease the number of variables in such a complicated system and to avoid problems of local convergence, the approximation of "hard helical cores" (backbones) and "soft shells" (side chains) for each helix was applied; the dihedral angles of backbones (but not those of side chains) were fixed at the values obtained by energy calculations for the individual TM helices. As judged by the X-ray structures of rhodopsin and bacteriorhodopsin, direct interactions between elements of the peptide backbone are essentially absent in the TM bundles of these proteins. Energy minimization that started from the global parameters corresponding to that of the PDB entry 1F88 yielded the 3D structure differing from 1F88 by the rms value of 1.81 Å (C^α-atoms only) using the energy convergence criterion of $\Delta E \leqslant 1$ kcal/mol. One run of energy minimization for a typical TM bundle required ca. 6 h at the single node PC with a 2.8 GHz processor under the Linux operational system.

Simplified energy-based scoring function. We also employed a more simplified energy calculation, where energy minimization was performed only in the space of global parameters (though the values of the dihedral angles of side chains were still optimized prior to each cycle of energy minimization). In this case, energies of atom–atom interactions within each individual helix were not included in the total energy values, so the resulting target function represents only inter-helical, but not intra-helical, interactions. Therefore, this function should be regarded as energy-based scoring function rather than as "real" energy. One run of the simplified calculations required up to 3–4 min.

Results and discussion

Constitutively active mutants of rhodopsin

Activation of rhodopsin is associated with 11-*cis*–*all trans* isomerization of retinal, which occurs as a result of exposure of the *cis*-retinal in rhodopsin to light. To our knowledge, there are only a few mutants of rhodopsin showing basal activity in dark, i.e., in presence of 11-*cis* retinal. All of them are double mutants combining mutations of M257 with substitutions presumably disrupting the salt bridge existing in the dark-adapted state between the nitrogen of the Schiff base attached to K296 and the unprotonated side chain of E113 [13,14]. The most potent CAM reported was E113Q/M257Y that in dark showed ca. 70% of functional activity of that of the light-adapted rhodopsin [14] or ca. 39% of functional activity it displayed when exposed to light [13]. The G90D/M257Y mutant also demonstrated pronounced basal activity in dark that was ca. 40% of functional activity of that of light-activated rhodopsin [14]. Two less pronounced CAMs, E113Q/M257N and E113Q/M257A, showed ca. 20% and 18% of functional activity they displayed when exposed to light, respectively [13]. None of the rhodopsin mutants with single modifications, as G90D, E113Q. M257Y, M257N or M257A, showed constitutive activity [13,14]; however, all of them displayed constitutive activity in absence of retinal, i.e., as mutants of opsin [13,38,39]. Interestingly, the opsin mutants with modification of M257 showed an order of displayed basal activities as M257Y > M257N > M257N, in agreement with the same order for the double mutants E113Q/M257Y, E113Q/M257N, and E113Q/M257A [13].

Energy calculations allow discrimination of R from R in CAMs of rhodopsin*

Our main hypothesis suggested that the R* state possesses an energy lower than that of the R state for pronounced CAMs. Our energy calculations, however, were deliberately limited by numerous simplifications. First, we considered only the TM bundle and not the entire receptor molecule. Second, no molecular environment, explicit lipids, water molecules, etc., was included in the calculations. Third, we employed a "hard core" and "soft shell" model of the TM bundle. These simplifications inevitably influence the accuracy of calculated energies of different configurations. Therefore, assuming that the R and R* states in rhodopsin mutants are roughly the same as in rhodopsin itself (i.e., for R all $\Delta Tx = 0°$, and for R* all $\Delta Tx = 0°$, except $\Delta Tx_6 = 120°$), the first question to answer was whether the values of calculated energies of configurations could discriminate between the R and R* states despite the multiple simplifications.

In this regard, Fig. 1 depicts differences in calculated energies between the R and R* states for non-CAM mutants, as G90D, E113Q, and M257Y, for pronounced CAMs, as G90D/M257Y and E113Q/M257Y, and for less pronounced CAMs, as E113Q/M257N and E113Q/M257A. Evidently, the R* states for the double mutants G90D/M257Y and E113Q/M257Y possessed significantly lower energies than the corresponding R states, not seen for the single mutants G90D, E113Q, and M257Y, which did not display constitutive activity in dark. The differences were also not characteristic for the less pronounced CAMs, such as E113Q/M257N and E113Q/M257A.

Thus, energy calculations performed according to the procedure described above were able to distinguish between rough 3D models of the R and R* states for pronounced CAMs and non-CAMs of rhodopsin. The second question to answer was whether it was possible to determine all configurations (all combinations of rotations of TM helices along the long transmembrane axes) with energies lower than that of the rhodopsin-like R state that, according to our hypothesis, may be the more likely

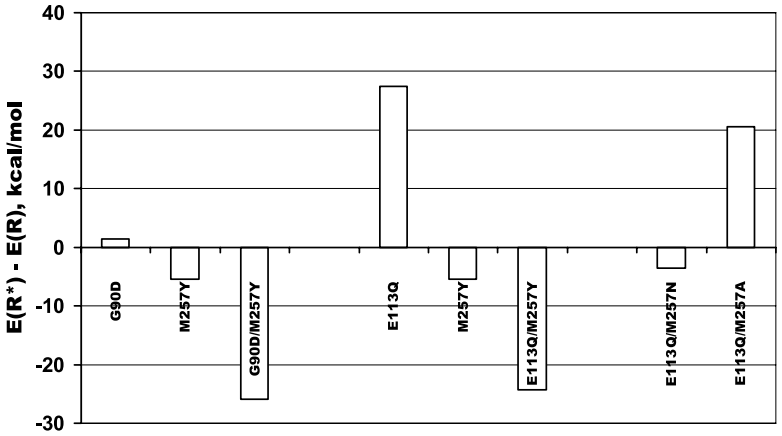

Fig. 1. Energy differences (in kcal/mol) between configurations of the TM bundle corresponding to the R and R* states of rhodopsin mutants.

candidates for the R* state of the mutants G90D/M257Y and E113Q/M257Y.

The build-up approach to sample the configurational space of helical packing in TM bundles

The complete sampling of possible rotations of the TM helices along the long transmembrane axes would involve all combinations of ΔTx values, chosen on some grid, for all seven TM helices. The total number of combinations with the reasonable grid step of 30° would then amount to $12^7 = 35{,}831{,}808$ configurations; obviously, considering all these combinations is far beyond our available computational resources. Fortunately, we have to search only for configurations that are of energies lower or at least comparable with that of the rhodopsin-like R state. It means that combinations of the ΔTx values that yield energies noticeably higher than the configuration corresponding to the R state may be removed from further considerations even in the case of interaction of only three contacting helices. This consideration allowed a build-up procedure, which significantly reduces amount of calculations by truncating the combinatorial explosion of energetically unfeasible substructures without damaging the general quality of configurational sampling.

At the first step of the build-up procedure, we may align individual TM helices to the X-ray structure of rhodopsin to obtain the global coordinates for the reference structure, where all $\Delta Tx = 0°$. Then, we may use an observation that not all TM helices tightly interact with each other in the X-ray structures of rhodopsin. Specifically, the tightest interactions are within the five "triplets" TM1-TM2-TM7, TM2-TM3-TM7, TM3-TM4-TM5, TM3-TM5-TM6, and TM3-TM6-TM7. To reduce number of configurations considered for triplets, the rotations of TM helices, which expose polar residues in the middle of the TM fragments (as N55, T58, N78, D83, T92, E113, T118, E122, S127, T160, C167, H211, C222, and C264) to lipids, may be excluded from consideration as possible starting points. (The polar residues that are located closer to the ends of the TM fragments may interact with polar heads of phospholipids.) Also, rotations of TM7 in the rhodopsin mutants are not likely, since this TM helix is connected directly with the H8 helix that is bound to the intracellular membrane surface [5].

Energy calculations for triplets may allow selection of configurations with relative energies not higher than that of the reference structure, E_R, according to some energy cut-off. Then these configurations of the triplets could be combined in the packages of the four contacting helices, TM1-TM2-TM3-TM7, TM2-TM3-TM6-TM7, TM3-TM5-TM6-TM7, and TM3-TM4-TM5-TM6. After a new round of energy calculations and selection, the newly selected configurations could be combined into packages of five contacting helices and so on until the entire TM bundle was built. Obviously, there is a possibility that configurations of triplets discarded on the ground of their high relative energies may correspond to configurations with low relative energies in the packages of the four contacting helices, and so on. This problem, however, could be resolved by proper selection of the energy cut-off values at each sequential step of the procedure.

Identification of the likely 3D models of the R state for the CAMs of rhodopsin*

Table 1 describes the actual steps of the procedure performed for the G90D/M257Y and E113Q/M257Y mutants. The starting values of ΔTx's were, generally, those chosen on the grid of 30°; for some helices, however, some starting points on the grid were omitted, since they corresponded to rotations that expose polar TM residues to the membrane environment, as mentioned above. Specifically, only starting points of 0°, 30°, 60°, 90°, 240°, 270°, 300°, and 330° were chosen for ΔTx_1; 0°, 30°, 60°, 90°, 120°, 270°, 300°, and 330° for ΔTx_4; 0°, 30°, 60°, 90°, and 330° for ΔTx_5 and 0°, 30°, 60°, 90°, 120°, 150°, 180°, and 330° for ΔTx_6. Table 1 lists mutants for which calculations were performed in each case; numbers of the starting combinations; numbers of the selected combinations; and the values of ΔTx's that remained for further consideration, if they were different from the starting values. The

Table 1
Subsequent steps of the build-up procedure exploring possible combinations of rotations of TM helices along the long axes in G90D/M257Y and E113Q/M257Y

TM helices	Mutant	Number of starting combinations of ΔTx's	Number of selected combinations of ΔTx's	ΔTx values selected for further consideration
127	G90D	96	17	ΔTx_2: 0, 30, 60, 120
237	G90D E113Q	48	25	
367	E113Q M257Y E113Q/M257Y	96	32	ΔTx_3: 0, 60, 90, 120, 150, 210, 240, 270, 300, 330
356	E113Q M257Y E113Q/M257Y	400	205	
345	E113Q	400	269	
3567	E113Q/M257Y	96	20	ΔTx_3: 0, 210, 240, 300, 330 ΔTx_6: 0, 120, 150, 330
2367	G90D/M257Y E113Q/M257Y	19	3	ΔTx_2: 0 ΔTx_3: 0 ΔTx_6: 0, 120, 150
1237	G90D/M257Y E113Q/M257Y	7	6	
3456	E113Q/M257Y	85	59	
34567	E113Q/M257Y	43	27	
12367	G90D/M257Y	18	18	
234567	G90D/M257Y	27	11	
1234567	G90D/M257Y E113Q/M257Y	66	11	

order of the steps corresponded to the order of rows in Table 1. For each next step, starting combinations of ΔTx's were those selected by energy calculations for all mutants considered at the previous step. Since packages of only three helices lack many important interactions with other helices, results of applying full energy minimization for triples may be misleading showing, for example, the total predominance of a single configuration in the TM1-TM2-TM7 triple (data not shown). Therefore, energy calculations for packages of three helices were performed using a much more permissive energy-based scoring function (see Methods) and employed the energy cut-off of $E(\mathrm{R}) - E_i \leqslant 5$ kcal/mol for selection of combinations of ΔTx's for further consideration. In all other cases, full energy minimization was applied, and the energy cut-off of 25 kcal/mol was used.

Subsequent steps of the procedure resulted in 66 possible configurations of the entire TM bundle of rhodopsin. The configurations consisted of the same packages of the six helices (TM2, TM3, TM4, TM5, TM6, and TM7) for each of the six values of ΔTx_1, namely 0°, 30°, 240°, 270°, 300°, and 330°. Since our main interest was in comparing configurations of the TM bundle with the reference structure of the R state (all $\Delta Tx = 0°$), only 11 configurations corresponding to $\Delta Tx_1 = 0°$ were selected for consideration at the level of the entire TM bundle. They are listed in Table 2 according to the starting values of ΔTx's. Note that the values of all global

Table 2
Configurations of the entire TM bundle of rhodopsin subjected to energy calculations (starting ΔTx values and final energies relative to the R state, configuration 1)

#	ΔTx values							$E_i - E(\mathrm{R})$ kcal/mol	
	ΔTx_1	ΔTx_2	ΔTx_3	ΔTx_4	ΔTx_5	ΔTx_6	ΔTx_7	G90D/M257Y	E113Q/M257Y
1	0	0	0	0	0	0	0	0	0
2	0	0	0	120	0	0	0	27.07	−2.22
3	0	0	0	30	60	0	0	8.83	−5.54
4	**0**	**0**	**0**	**0**	**0**	**120**	**0**	**−25.96**	**−24.27**
5	0	0	0	60	0	120	0	3.13	−7.95
6	0	0	0	330	0	120	0	−2.77	−11.29
7	**0**	**0**	**0**	**0**	**30**	**120**	**0**	**−15.09**	**−20.49**
8	0	0	0	330	30	120	0	−2.06	23.05
9	0	0	0	330	60	120	0	−35.72	6.42
10	**0**	**0**	**0**	**270**	**330**	**120**	**0**	**−15.72**	**−23.00**
11	0	0	0	0	0	150	0	−5.77	−43.66

parameters, including ΔTx's, were not the same after energy minimization as the starting ΔTx's; however, practically in all cases they differ from each other by not more that ca. 10°–15°.

Energies for two of the selected configurations (numbers 1 and 4) that correspond to the R and R* states of the TM bundle have been calculated already (see Fig. 1). Table 2 lists results of energy calculations for all selected configurations of the entire TM bundles of G90D/M257Y and E113Q/M257Y (the results are also depicted in Fig. 2). Apart from configuration 4, two other configurations, namely 7 and 10, possessed relative energies distinctly lower than that of the R state for both constitutively active analogs, both being additional candidates for 3D models of the R* state of rhodopsin (all three configurations are shown in bold in Table 2). In fact, the three configurations are similar to each other, all corresponding to ΔTx_6 of 120° and ΔTx_5 of $0° \pm 30°$. The only difference is in rotation of TM4 in configuration 10 compared to configurations 4 and 7 (ΔTx_4 of 270° instead of 0°). However, helix TM4 is the one least involved in interactions between TM helices, and its rotation cannot really affect rotation of TM6 by ca. 120° occurring upon transition from the R state to R* state. Besides, the available experimental data do not specify changes in the position of TM4 in rhodopsin in the dark-adapted vs. light-activated state (see, e.g., [10]). Thus, our approach that sampled all reasonable combinations of rotations of the TM helices along their long axes for two constitutively active mutants of rhodopsin correctly predicted the main features of the 3D models for the R* state of rhodopsin, in good agreement with the actual 3D model for the R* state suggested by experiment.

Inter-residue interactions in constitutively active mutants of rhodopsin

It would be difficult to assign any significant differences between the energies corresponding to the R and R* states of the CAMs and non-CAMs of rhodopsin to any single specific inter-residue interaction. Energy calculations, however, revealed some general features of the balance of residue–residue interactions in the non-constitutively active single mutants G90D, E113Q or M257Y and the constitutively active double mutants G90D/M257Y and E113Q/M257Y. In agreement with the common suggestion (e.g., [14,40,41]), the calculations showed that mutations E113Q or G90D result in weakening the interaction between TM3 and TM7 due to decreasing of favorable electrostatic interaction between the residue in position 113 and the nitrogen of the Schiff base connected to retinal (position 296). While it occurs due to elimination of the negative charge in position 113 in the E113Q mutant, in the G90D mutant it is a consequence of competition for interaction with this nitrogen by the side chain of D90 (see Fig. 3 showing configuration 4 for G90D/M257Y). Our calculations showed also that the hydroxyl of the T94 side chain was involved in the hydrogen bonding either with the backbone carbonyl of the residue in position 90 or with the side chain of the residue in position 113. The former H-bond was observed in the R state for all mutants, and the latter one was observed in the R* states in the E113Q and M257Y mutants (but not in the double mutants). This finding emphasizes the importance of residue T94 in the balance of transmembrane helical interactions. It is noteworthy that mutants G90D, E113Q, and T94I are the known CAMs of opsin in the absence of retinal [39,38,42]; these mutations are also considered to be the possible cause of congenital night blindness [39,42,43]. In rhodopsin, however, those mutations alone do not result in preference of the R* state over the R state, though they facilitate some slight movements of TM3 as a rigid body and some rearrangements of the TM3 side chains that are unavailable in the wild type rhodopsin. On the other hand, energy calculations showed changes in interaction between residues R135 and Y257 in the mutants with the M257Y mutation compared to that between R135 and M257. In the R* state, this interaction influences the spatial position of R135 causing additional strengthening of the

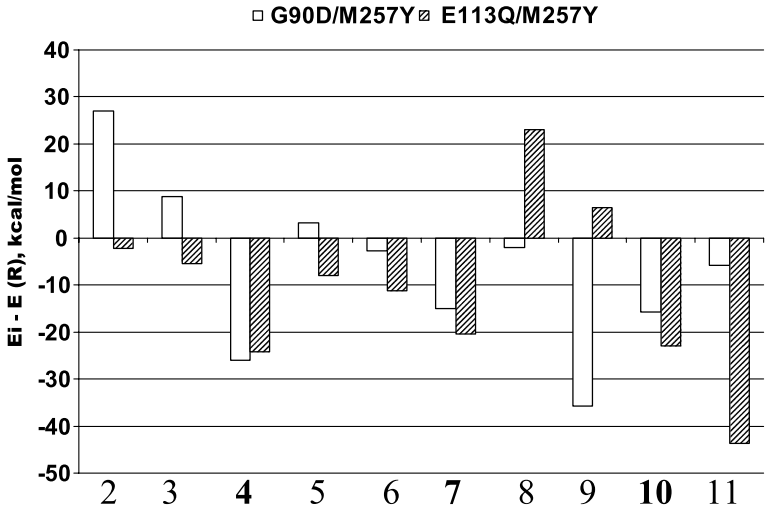

Fig. 2. Differences between energies of a given configuration (see numbering at the bottom) and that of the R state for G90D/M257Y and E113Q/M257Y.

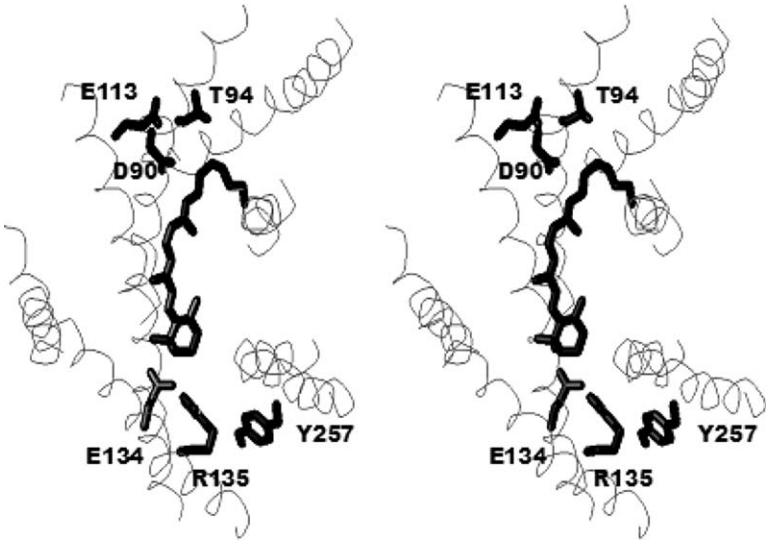

Fig. 3. Stereosketch of the suggested R* state of G90D/M257Y mutant displaying side chains of D90, T94, E113, E134, R135, Y257, and K296 with the attached 11-*cis* retinal. TM helices are shown as one-line ribbons. View is from the extracellular side of the membrane approximately parallel to the TM7 long axis.

salt bridge between the side chains of E134 and R135 residues in TM3. Combined with small, but important, changes between the R and R* states initiated by the G90D or E113Q mutations, this specific difference, which affects the highly conserved fragment D/ERY in TM3, contributes to the energetic preference of the R* state over the R state in the double mutants G90D/M257Y and E113Q/M257Y.

Concluding remarks

This study suggested a modeling approach for fast and efficient elucidation of possible 3D models of the TM region for the activated states of the rhodopsin-like GPCRs that differ from the resting state by rotations of the TM helices along their transmembrane axes. The approach involves comprehensive sampling in configurational space of helical packing of the TM bundle employing a simple and robust computational build-up procedure. The main hypothesis was that the 3D models for the activated states should correspond to the configurations of the TM bundle with relative energies lower than those for the resting state for pronounced CAMs but not for non-CAMs.

The hypothesis was tested in the case of rhodopsin, the only GPCR for which direct structural data on the R and R* states are currently available. Despite simplifications of modeling (employment of the ECEPP force field assuming rigid valence geometry; absence of membrane environment, water and ions; fixing dihedral angles of backbone in TM helices during the packing procedure, etc.), energy calculations showed that relative energies for the R* state in the pronounced constitutively active double mutants of rhodopsin G90D/M257Y and E113Q/M257Y are significantly lower than the energies for the R state, contrary to results obtained for the non-constitutively active single mutants G90D, E113Q, and M257Y. The developed build-up procedure successfully identified few similar configurations of the TM helical bundle of G90D/M257Y and E113Q/M257Y as possible candidates for the 3D model of the R* state of rhodopsin, all of them being in good agreement with the model suggested by experiment. Since constitutively active mutants are known for many of GPCRs belonging to the large rhodopsin-like family, this approach can be used to predict possible 3D structures corresponding to the activated states of the TM regions of many GPCRs. The predicted structures may be then refined by applying more sophisticated modeling approaches (such as molecular dynamics studies involving detailed description of molecular environment), as well as subjected to final validation by appropriate experimental procedures.

Acknowledgment

The work was partly supported by NIH Grant GM 068460.

References

[1] U. Gether, Uncovering molecular mechanisms involved in activation of G protein-coupled receptors, Endocr. Rev. 21 (2000) 90–113.
[2] R. Fredriksson, M.C. Lagerstrom, L.G. Lundin, H.B. Schioth, The G-protein-coupled receptors in the human genome form five main families. Phylogenetic analysis, paralogon groups, and fingerprints, Mol. Pharmacol. 63 (2003) 1256–1272.
[3] J. Drews, Drug discovery: a historical perspective, Science 287 (2000) 1960–1964.
[4] C. Parnot, S. Miserey-Lenkei, S. Bardin, P. Corvol, E. Clauser, Lessons from constitutively active mutants of G protein-coupled receptors, Trends Endocrinol Metab. 13 (2002) 336–343.
[5] K. Palczewski, K. Takashi, H. Tetsuya, C. Behnke, H. Motoshima, B. Fox, I. Le Trong, D. Teller, T. Okada, R. Stenkamp, M. Yamamoto, M. Miyano, Crystal structure of rhodopsin: a G-protein-coupled receptor, Science 289 (2000) 739–745.

[6] D.C. Teller, T. Okada, C.A. Behnke, K. Palczewski, R.E. Stenkamp, Advances in determination of a high-resoultion three-dimensional structure of rhodpsin, a model of G-protein-coupled receptors (GPCRs), Biochemistry 40 (2001) 7761–7772.
[7] T. Okada, Y. Fujiyoshi, M. Silow, J. Navarro, E.M. Landau, Y. Shichida, Functional role of internal water molecules in rhodopsin revealed by X-ray crystallography, Proc. Natl. Acad. Sci. USA 99 (2002) 5982–5987.
[8] J. Li, P.C. Edwards, M. Burghammer, C. Villa, G.F. Schertler, Structure of bovine rhodopsin in a trigonal crystal form, J. Mol. Biol. 343 (2004) 1409–1438.
[9] T. Okada, M. Sugihara, A.N. Bondar, M. Elstner, P. Entel, V. Buss, The retinal conformation and its environment in rhodopsin in light of a new 2.2 Å crystal structure, J. Mol. Biol. 342 (2004) 571–583.
[10] W.L. Hubbell, C. Altenbach, H.G. Khorana, Rhodopsin structure, dynamics and activation, Adv. Protein Chem. 63 (2003) 243–290.
[11] J.J. Ruprecht, T. Mielke, R. Vogel, C. Villa, G.F. Schertler, Electron crystallography reveals the structure of metarhodopsin I, EMBO J. 23 (2004) 3609–3620.
[12] J.M. Kim, C. Altenbach, R.L. Thurmond, H.G. Khorana, W.L. Hubbell, Structure and function in rhodopsin: rhodopsin mutants with a neutral amino acid at E134 have a partially activated conformation in the dark state, Proc. Natl. Acad. Sci. USA 94 (1997) 14273–14278.
[13] M. Han, S.O. Smith, T.P. Sakmar, Constitutive activation of opsin by mutation of methionine 257 on transmembrane helix 6, Biochemistry 37 (1998) 8253–8261.
[14] J.M. Kim, C. Altenbach, M. Kono, D.D. Oprian, W.L. Hubbell, H.G. Khorana, Structural origins of constitutive activation in rhodopsin: role of the K296/E113 salt bridge, Proc. Natl. Acad. Sci. USA 101 (2004) 12508–12513.
[15] J.A. Ballesteros, L. Shi, J.A. Javitch, Structural mimicry in G protein-coupled receptors: implications of the high-resolution structure of rhodopsin for structure–function analysis of rhodopsin-like receptors, Mol. Pharmacol. 60 (2001) 1–19.
[16] D.L. Farrens, C. Altenbach, K. Yang, W.L. Hubbell, H.G. Khorana, Requirement of rigid-body motion of transmembrane helices for light activation of rhodopsin, Science 274 (1996) 768–770.
[17] U. Gether, S. Lin, P. Ghanouni, J.A. Ballesteros, H. Weinstein, B.K. Kobilka, Agonists induce conformational changes in transmembrane domains III and VI of the beta2 adrenoceptor, EMBO J. 16 (1997) 6737–6747.
[18] A.D. Jensen, F. Guarnieri, S.G. Rasmussen, F. Asmar, J.A. Ballesteros, U. Gether, Agonist-induced conformational changes at the cytoplasmic side of transmembrane segment 6 in the beta 2 adrenergic receptor mapped by site-selective fluorescent labeling, J. Biol. Chem. 276 (2001) 9279–9290.
[19] S.P. Sheikh, J.P. Vilardarga, T.J. Baranski, O. Lichtarge, T. Iiri, E.C. Meng, R.A. Nissenson, H.R. Bourne, Similar structures and shared switch mechanisms of the beta2-adrenoceptor and the parathyroid hormone receptor. Zn(II) bridges between helices III and VI block activation, J. Biol. Chem. 274 (1999) 17033–17041.
[20] I. Sylte, A. Bronowska, S.G. Dahl, Ligand induced conformational states of the 5-HT(1A) receptor, Eur. J. Pharmacol. 416 (2001) 33–41.
[21] D.A. Shapiro, K. Kristiansen, D.M. Weiner, W.K. Kroeze, B.L. Roth, Evidence for a model of agonist-induced activation of 5-hydroxytryptamine 2A serotonin receptors that involves the disruption of a strong ionic interaction between helices 3 and 6, J. Biol. Chem. 277 (2002) 11441–11449.
[22] H.G. Khorana, Molecular biology of light transduction by the mammalian photoreceptor, rhodopsin, J. Biomol. Struct. Dyn. 11 (2000) 1–16, Conversation.
[23] C.E. Elling, K. Thirstrup, B. Holst, T.W. Schwartz, Conversion of agonist site to metal-ion chelator site in the beta(2)-adrenergic receptor, Proc. Natl. Acad. Sci. USA 96 (1999) 12322–12327.
[24] B. Holst, C.E. Elling, T.W. Schwartz, Partial agonism through a zinc-ion switch constructed between transmembrane domains III and VII in the tachykinin NK(1) receptor, Mol. Pharmacol. 58 (2000) 263–270.
[25] J.E. Porter, D.M. Perez, Characteristics for a salt-bridge switch mutation of the alpha(1b) adrenergic receptor. Altered pharmacology and rescue of constitutive activity, J. Biol. Chem. 274 (1999) 34535–34538.
[26] B.O. Gerber, E.C. Meng, V. Dotsch, T.J. Baranski, H.R. Bourne, An activation switch in the ligand binding pocket of the C5a receptor, J. Biol. Chem. 276 (2001) 3394–3400.
[27] D. Donnelly, S. Maudsley, J.P. Gent, R.N. Moser, C.R. Hurrell, J.B. Findlay, Conserved polar residues in the transmembrane domain of the human tachykinin NK2 receptor: functional roles and structural implications, Biochem. J. 339 (1999) 55–61.
[28] C. Govaerts, A. Lefort, S. Costagliola, S.J. Wodak, J.A. Ballesteros, J. Van Sande, L. Pardo, G. Vassart, A conserved Asn in transmembrane helix 7 is an on/off switch in the activation of the thyrotropin receptor, J. Biol. Chem. 276 (2001) 22991–22999.
[29] S. Miura, S.S. Karnik, Constitutive activation of angiotensin II type 1 receptor alters the orientation of transmembrane helix-2, J. Biol. Chem. 277 (2002) 24299–24305.
[30] P.S. Crozier, M.J. Stevens, L.R. Forrest, T.B. Woolf, Molecular dynamics simulation of dark-adapted rhodopsin in an explicit membrane bilayer: coupling between local retinal and larger scale conformational change, J. Mol. Biol. 333 (2003) 493–514.
[31] B. Borhan, M.L. Souto, H. Imai, Y. Shichida, K. Nakanishi, Movement of retinal along the visual transduction path, Science 288 (2000) 2209–2212.
[32] G.V. Nikiforovich, G.R. Marshall, 3D Model for meta-II rhodopsin, an activated G-protein-coupled receptor, Biochemistry 42 (2003) 9110–9120.
[33] L.G. Dunfield, A.W. Burgess, H.A. Scheraga, Energy parameters in polypeptides. 8. Empirical potential energy algorithm for the conformational analysis of large molecules, J. Phys. Chem. 82 (1978) 2609–2616.
[34] G. Nemethy, M.S. Pottle, H.A. Scheraga, Energy parameters in polypeptides. 9. Updating of geometrical parameters, nonbonded interactions, and hydrogen bond interactions for the naturally occuring amino acids, J. Phys. Chem. 87 (1983) 1883–1887.
[35] E. Pebay-Peyroula, G. Rummel, J.P. Rosenbush, E.M. Landau, X-ray structure of bacteriorhodopsin at 2.5 angstroms from microcrystals grown in lipidic cubic phases, Science 277 (1997) 1676–1681.
[36] J. Deisenhofer, O. Epp, I. Sinning, H. Michel, Crystallographic refinement at 2.3 Å resolution and refined model of the photosynthetic reaction centre from *Rhodopseudomonas viridis*, J. Mol. Biol. 246 (1995) 429–457.
[37] G.V. Nikiforovich, V.J. Hruby, O. Prakash, C.A. Gehrig, Topographical requirements for delta-selective opioid peptides, Biopolymers 31 (1991) 941–955.
[38] P.R. Robinson, G.B. Cohen, E.A. Zhukovsky, D.D. Oprian, Constitutively active mutants of rhodopsin, Neuron 9 (1992) 719–725.
[39] V.R. Rao, G.B. Cohen, D.D. Oprian, Rhodopsin mutation G90D and a molecular mechanism for congenital night blindness, Nature 367 (1994) 639–642.
[40] V.R. Rao, D.D. Oprian, Activating mutations of rhodopsin and other G protein-coupled receptors, Annu. Rev. Biophys. Biomol. Struct. 25 (1996) 287–314.
[41] T.P. Sakmar, S.T. Menon, E.P. Marin, E.S. Awad, Rhodopsin: insights from recent structural studies, Annu. Rev. Biophys. Biomol. Struct. 31 (2002) 443–484.
[42] A.K. Gross, V.R. Rao, D.D. Oprian, Characterization of rhodopsin congenital night blindness mutant T94I, Biochemistry 42 (2003) 2009–2015.
[43] S. Jin, M.C. Cornwall, D.D. Oprian, Opsin activation as a cause of congenital night blindness, Nat. Neurosci. 6 (2003) 731–735.